VOL. 11, NO. 2, JANUARY 2016 ISSN 1819-6608
ARPN Journal of Engineering and Applied Sciences

www.arpnjournals.com

MODELING AND SIMULATION OF MODIFIED BRIDGELESS CONVERTER AND A SINGLE PHASE SEVEN-LEVEL INVERTER FOR A SOLAR POWER GENERATION SYSTEM

J. Sevugan Rajesh[1] and R. Revathi[2]
[1]Electrical and Electronics Engineering Department, Kalaivani College of Technology, Coimbatore, India
[2]Electrical and Electronics Engineering Department, KPR Institute of Engineering and Technology, Coimbatore, India
E-Mail: sevugan.rajesh@gmail.com

ABSTRACT

This paper proposes a solar power generation system, which integrates a modified bridge less converter and a new seven-level inverter with a novel pulse width modulation (PWM) control scheme. High static gain step-up dc-dc converter based on the modified SEPIC converter with magnetic coupling and without magnetic coupling are presented and analyzed. The dc–dc converter to specify the size of incremental current in the current command of MPPT. This proposed seven- level inverter is designed using a capacitor selection circuit and a bridgeless power converter, connected in cascade. Proper switching of the inverter can produce seven output-voltage levels (Vdc, 2Vdc /3, Vdc /3, 0,−Vdc, −2Vdc /3, −Vdc /3) from the dc supply voltage. The performance of the proposed maximum power point tracker and seven-level inverter are demonstrated in MATLAB simulation at different operating conditions.

Keywords: DC/DC converter, multilevel inverter, pulse-width modulated inverter.

INTRODUCTION

India and China are the two countries responsible for major consumption of energy. The usage of coal will increase to about 80 percent by 2030. This in turn results in increased CO2 emission thereby polluting the environment. Thus, solar energy is becoming more important since it produces less pollution and the cost of fossil fuel energy is rising, while the cost of PV arrays is decreasing. Photovoltaic (PV) systems are considered to be one of the most resourceful and well-customary renewable energy sources because of their suitability in distributed generation, mobile applications, etc.

PV systems suffer from a major drawback which is the nonlinearity between the output voltage and current particularly under partially shaded conditions. However, the development for improving the competence of the PV system is still a demanding field of research. Generally, MPPT is adopted to track the maximum power point in the PV system. The P&O Maximum Power Point Tracking algorithm is mostly used because of its simple structures and fewer parameters. The conversion power is importantto solar power generation systems because it converts the dc power generated by a PV array into ac power and feeds this ac power into the utility grid.

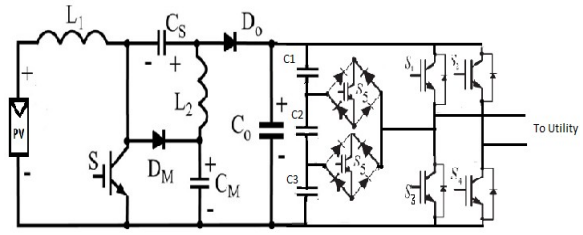

Figure-1. Circuit configuration of single-phase seven-inverter for photovoltaic systems.

The Types of inverter technology for connecting photovoltaic (PV) modules to a single-phase grid has been investigate [3]. The three-level inverter can suit specifications through its very high switching, but it could also regrettably increase switching losses, acoustic noise, and level of intervention to other equipment. Multilevel inverters are advantageous increasing the number of voltage levels in the inverter and distinctive structure of multilevel voltage source inverters allows them to achieve high voltages with low harmonics without the use of transformers. The harmonic content of the output voltage waveform that are better than those of conventional two-level inverters, also lower EMI, and requires smaller filter size, all of which make them low cost, less weight, and more compact [4], [5]. The term multilevel began with the three-level converter. Subsequently, several multilevel converter topologies have been developed. Common ones are diode- clamped [6]–[7], flying capacitor or multicell [8]–[9], and modified H-bridge multilevel [10]. This paper recounts the progress of a novel modified H-bridge single-phase multilevel inverter that has two diode surrounded bidirectional switches and a novel pulse width modulated (PWM) technique. The topology was useful to a photovoltaic system with considerations for a maximum-power-point tracker (MPPT). The proposed single-phase seven-level inverter was constructed from the five-level inverter [10].

BRIDGELESS DC–DC POWER CONVERTER

As seen in Figure-1, the SEPIC converter is composed of inductor L1, L2 a power electronic switch Q1 Capacitor Cs, and a diode, D0[9].

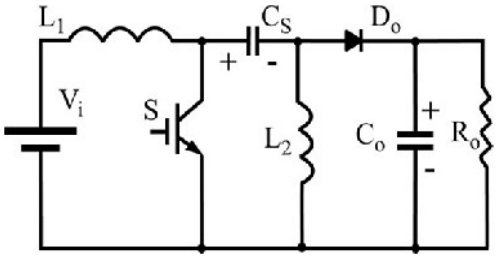

Figure-2. Classical SEPIC converter.

A SEPIC is essentially a boost converter followed by a buck-boost converter, therefore it is similar to a traditional buck-boost converter, but has advantages of having non-inverted output, using a series capacitor to couple energy from the input to the output and being capable of true shutdown. When the switch is turned off, its output drops to 0 V, following a fairly hefty transient dump of charge. The output voltage of the SEPIC is controlled by the duty cycle of the MOSFET. SEPIC is useful in applications like battery charging where voltage can be above and below that of the regulator output.

PROPOSED DC-DC CONVERTER WITHOUT MAGNETIC COUPLING

The power circuit of the classical SEPIC converter is presented in Figure-4. The modification of the SEPIC converter is accomplished adding only two components with the inclusion of the diode DM and the capacitor CM, as presented in Figure-4. Many operational characteristics of the classical SEPIC converter are changed with the proposed modification, as the elevation of the converter static gain. The capacitor CM is charged with the output voltage of the classical boost converter. The polarity of the CS capacitor voltage is inverted in the proposed converter. The continuous conduction mode (CCM) of the modified SEPIC converter presents two operation stages.

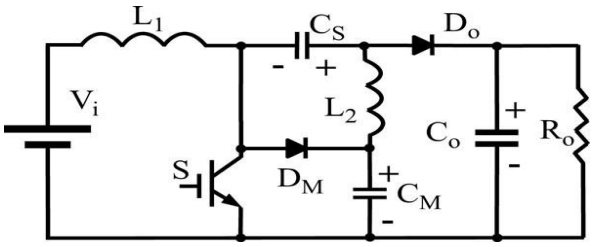

Figure-3. Modified SEPIC converter without magnetic coupling.

1) First stage [t0−t1] (Figure-4): At the instant t_0 , switch *S* is turned-off and the energy stored in the input inductor L_1 is transferred to the output through the C_S capacitor and output diode *Do* and also is transferred to the C_M capacitor through the diode D_M. Therefore, the switch voltage is equal to the C_M capacitor voltage. The energy stored in the inductor L_2 is transferred to the output through the Diode *Do*.

Second stage [t1−t2] (Figure-5): At the instant $t1$, switch *S* is turned-on and the diodes D_M and *Do* are blocked and the inductors $L1$ and $L2$ store energy. The input voltage is applied to the input inductor L_1 and the voltage $VC_S - VC_M$ is applied to the inductor L_2. The VC_M voltage is higher than the VCS voltage.

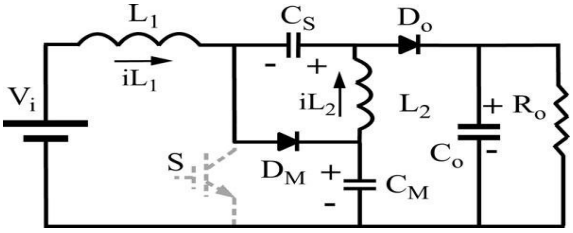

Figure-4. First stage of operation.

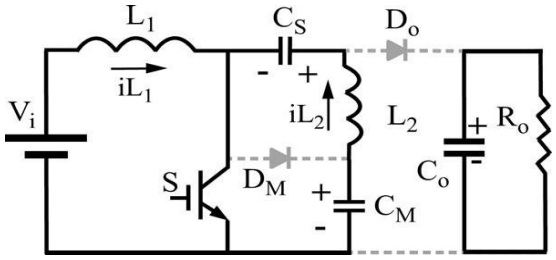

Figure-5. Second stage of operation.

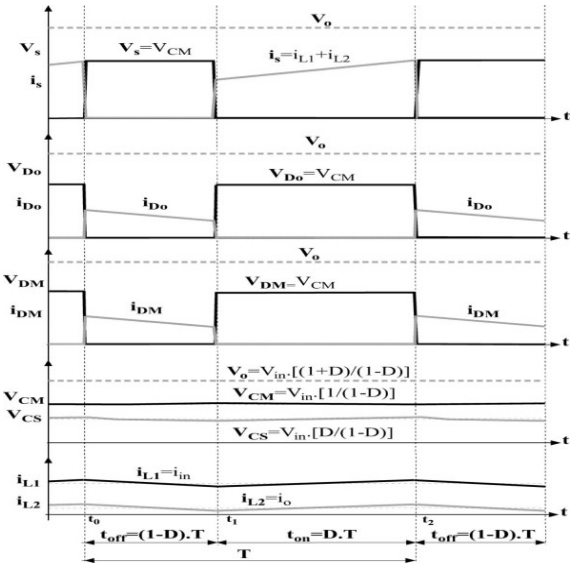

Figure-6. Theoretical waveform operating with hard switching commutation.

PROPOSED DC-DC CONVERTER WITH MAGNETIC COUPLING

The modified SEPIC converter without magnetic coupling can operate with the double of the static gain of the classical boost converter for a high Duty-cycle operation. However, in some applications very high static gain is necessary. A simple solution to elevate the static gain without increases the duty cycle is to include a

secondary winding in the L2 inductor. The secondary winding L2 inductor can increases the output voltage and operating as a flyback transformer. Figure-7 shows this alternative circuit. The inclusion of winding L2 causes the problem of overvoltage at the output diode Do. This overvoltage is not easily controlled with classical snubbers circuit.

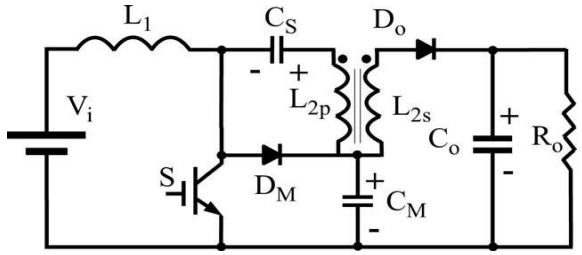

Figure-7. Proposed SEPIC converter with magnetic coupling.

A simple solution for this problem is the inclusion of a voltage multiplier at the secondary side as presented in Figure-8. This voltage multiplier consists of the diode DM2 and capacitor CS2 is also a clamping circuit for the output diode. The voltage multiplier increases the converter static gain, the voltage across the output diode is reduced to a value lower than the output voltage and the energy stored in the leakage inductance is transferred to the output.

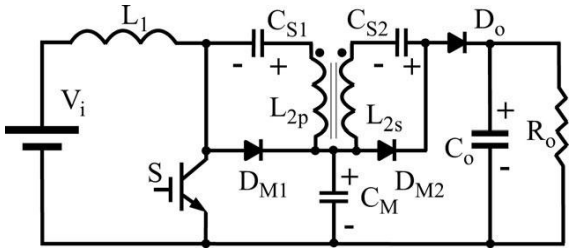

Figure-8. Proposed converter modified SEPIC converter with magnetic coupling and output diode voltage clamping.

This solutions based on the classical boost converter with magnetic coupling and the voltage multiplier cell can present very high voltage gain and an excellent performance as presented in [14]–[15]. The input current ripple is significantly increased and depends on the inductor winding turns ratio. As the magnetic coupling is not accomplished with the input inductor in the proposed topology, the input current ripple is low and is not changed by the magnetic coupling. There are also some proposed solutions based on the integration of the SEPIC converter with boost and flyback dc–dc converters. An isolated active clamp SEPIC-flyback converter is presented in [1] in order to obtain high efficiency. However, the proposed topology presents pulsating input current, and the active clamp technique increases the converter complexity with an additional controlled switch and command circuit.

The modified SEPIC converter with magnetic coupling in CCM operation presents five operation stages.

1) First stage [t0−t1] (Figure-9): The power switch S is conducting and the input inductor L1 stores energy. The capacitor CS2 is charged by the secondary winding L2S and diode DM2. The leakage inductance limits the current and the energy transference occurs in a resonant way. The output diode is blocked, and the maximum diode voltage is equal to (Vo−VCM). At the instant t1, the energy transference to the capacitor CS2 is finished and the diode DM2 is blocked.

2) Second stage [t1−t2] (Figure-10): From the instant t1 , when the diode DM2 is blocked, to the instant t2 when the power switch is turned OFF, the inductors L1 and L2 store energy and the currents linearly increase.

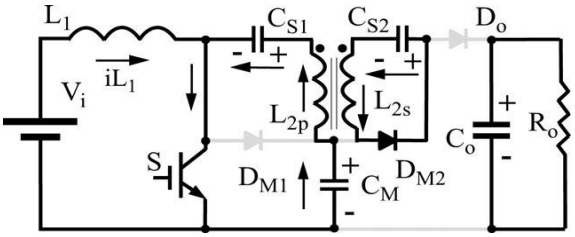

Figure-9. First stage of operation.

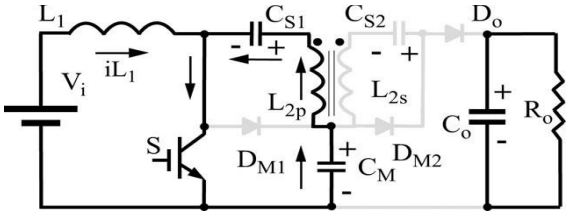

Figure-10. Second stage operation.

3) Third stage [t2−t3] (Figure-12): At the instant t2 the power switch S is turned OFF. The energy stored in the L1 inductor is transferred to the CM capacitor. Also, there is the energy transference to the output through the capacitors CS1, CS2 inductor L2 and output diode Do.

4) Fourth stage [t3−t4] (Figure-13): At the instant t3, the energy transference to the capacitor CM is finished and the diode DM1 is blocked. The energy transference to the output is maintained until the instant t4, when the power switch is turned ON.

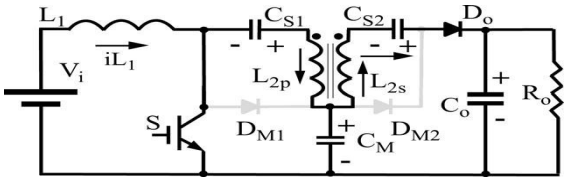

Figure-11. Third stage of operation.

5) Fifth stage [t4−t5] (Figure-14): When the power switch is turned ON at the instant t4, the current at the output diode Do linearly decreases and the di/dt is limited by the transformer leakage inductance, reducing the diode reverse recovery current problems. When the output diode is blocked, the converter returns to the first operation stage.

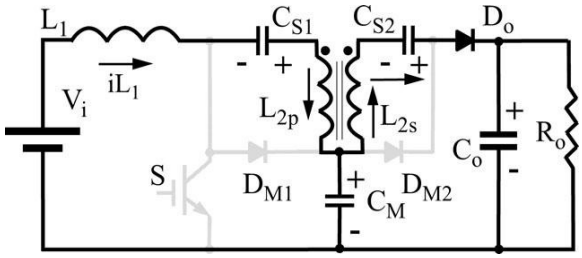

Figure-12. Fourth stage of operation.

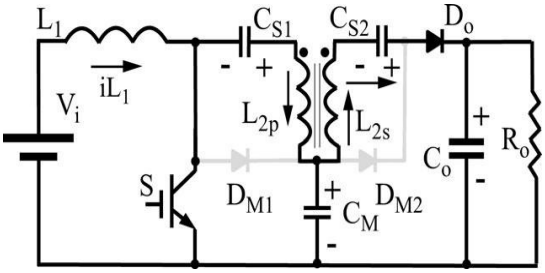

Figure-13. Fifth operation stage.

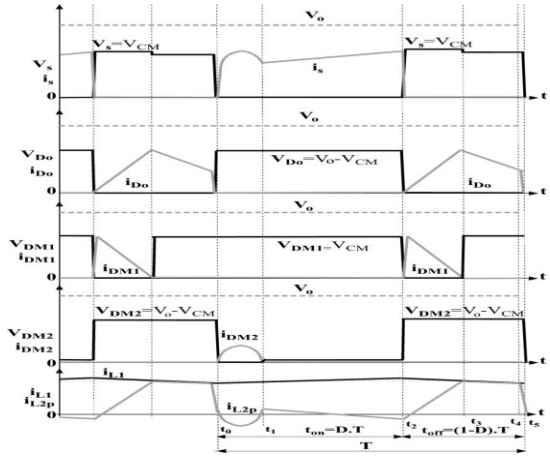

Figure-14. Theoretical waveform operating with hard switching commutation.

SEVEN-LEVEL INVERTER

The proposed single-phase seven-level inverter was developed from the five-level inverter in [25] – [29].Photovoltaic (PV) arrays were connected to the inverter via a dc–dc boost converter. High dc bus voltages are essential to promise that power flows from the PV arrays to the utility. By Proper switching of the inverter can make seven output-voltage levels (Vdc, 2Vdc /3, Vdc /3, 0, −Vdc, −2Vdc /3, −Vdc /3) from the dc supply voltage.

The seven switching states operation, of proposed inverter's as shown in Figure-15(a)–(g).

- Maximum positive output (Vdc): S1and S4 of the full-bridge power converters are ON. All the Remaining controlled switches are OFF. At this stage the voltage applied to the load terminals is Vdc. Figure-15(a) shows the current paths that are active at this stage.

- Two-third positive output (2Vdc /3): The bidirectional switch S5and S4 of the full-bridge power converter is ON, so C1 and C2 are discharged in series and the output voltage applied to the load terminals is 2Vdc /3. All other controlled switches are OFF; Figure-15(b) shows the current paths that are active at this stage.

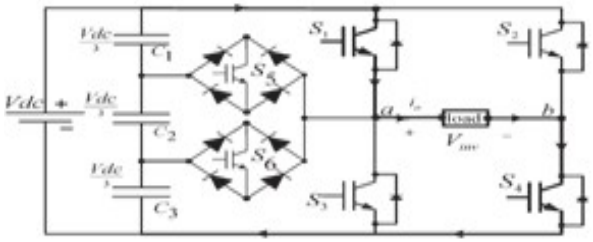

(a)

- One-third positive output (Vdc /3): The bidirectional switch S6 and S4 of the full-bridge power converter is ON, so C2 is discharged through S6 and S4 and the output voltage applied to the load terminals is 2Vdc /3. All other controlled switches are OFF; Figure-15(c) shows the current paths that are active at this stage.

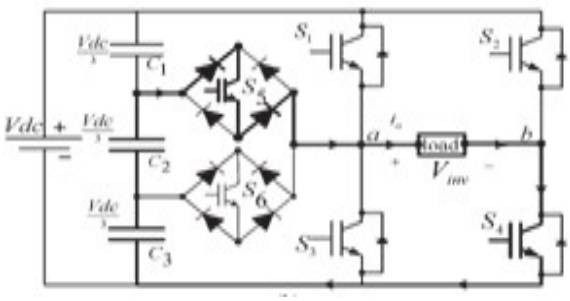

(b)

- Zero output: This level can be achieved by two switching combinations; switches S3 and S4 are ON, or S1 and S2 are ON, which short circuit the load terminal ab, and the voltage applied to the load terminals is zero. All other controlled switches are OFF; Figure-15(d) shows the current paths that are active at this stage.

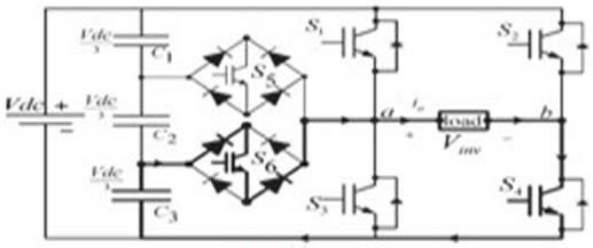

(c)

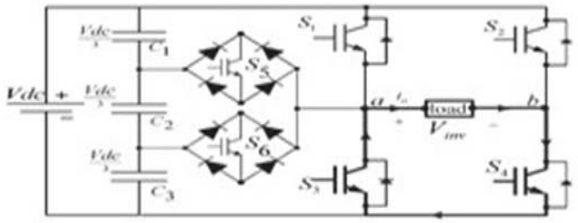

(d)

- One-third negative output (−Vdc /3): The bidirectional switch S5 and S2 of the full-bridge power converter is ON, so C1 is discharged through S2 and S5 and the output voltage applied to the load terminals is 2Vdc /3. All other controlled switches are OFF.

- Two-third negative output (−2Vdc /3): The bidirectional switch S6 and S2 of the full-bridge power converter is ON, so C1 and C2 are discharged in series and the output voltage applied to the load terminals is −2Vdc /3. Figure-15(f) shows the current paths that are active at this stage

- Maximum negative output (−Vdc): S2 and S3 of the full-bridge power converters are ON. S2 connects the load negative terminal to Vdc, and S3 connects the load positive terminal to ground. All other switches are OFF; the voltage applied to the load terminals is −Vdc. Figure-15(g) shows the current paths that are active at this stage.

PWM MODULATION

A new PWM modulation technique as introduced to make the PWM switching signals. Three reference signals (Vref1, Vref2, and Vref3) were compared with a carrier signal (Vcarrier). The reference signals had the same frequency and amplitude and were in phase with an offset value that was equivalent to the amplitude of the carrier signal. The each reference signals were compared with the carrier signal. The Vref1 was compared with Vcarrier until it exceeded the peak amplitude of Vcarrier. Vref2 would be compared until it reached zero, Once Vref3 had reached zero. Then, onward, Vref1 would be compared with Vcarrier. Figure-8 shows the resulting switching pattern. Switches S1, S3, S5, and S6 were switching at the rate of the carrier signal frequency, whereas S2 and S4 would operate at the fundamental frequency. For one cycle of the fundamental frequency, the proposed inverter operated through six modes.

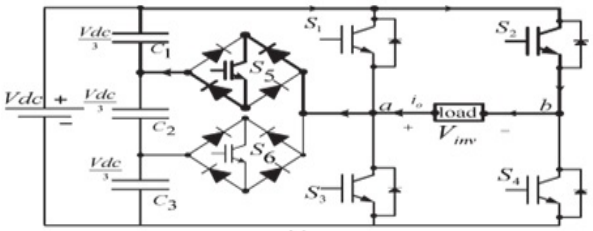

(e)

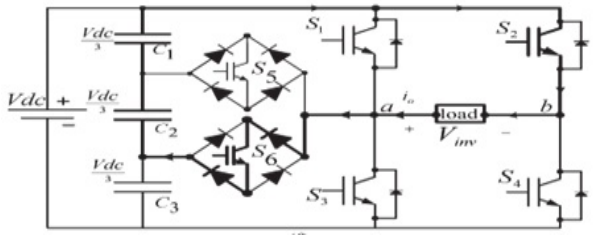

(f)

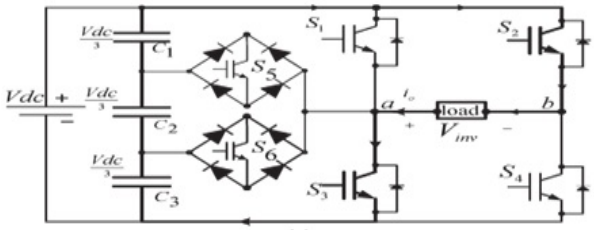

(g)

Figure-15. a, b, c, d, e, f, g, - Switching combination required to generate the output voltage (Vab). (e) Vab = $-V$dc/3. (f) $Vab=-2V$dc/3. (g) Vab = $-V$dc.

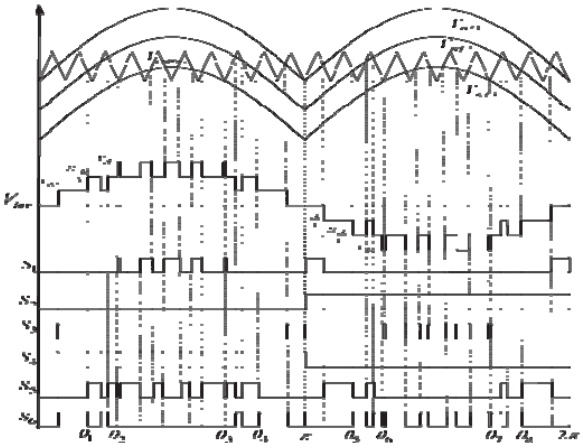

Figure-16. Switching pattern for the single-phase seven-level inverter.

RESULT AND DISCUSSIONS

The proposed scheme has been simulated in MATLAB/Simulink environment. The transient and steady state behavior of the modified SEPIC converter with magnetic coupling shows in Figure-17 and 18.

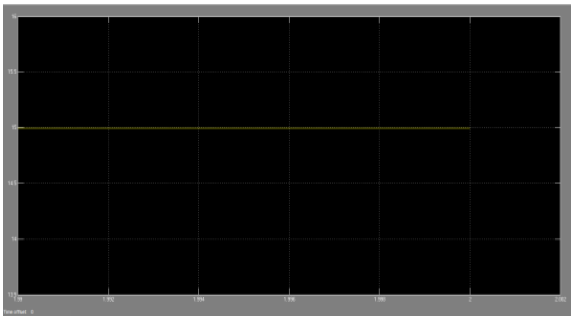

Figure-17. Vin (input voltage) vs. time for modified SEPIC converter with magnetic coupling.

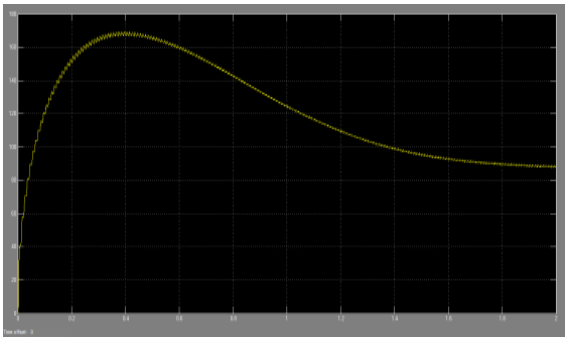

Figure-18. Vout (Output voltage) vs time for modified SEPIC converter with magnetic coupling.

Current and voltage waveforms of the proposed inverter circuit are shown in Figure-19 and Figure-20. Circuit shows that less number of switching devices is used which reduces the switching losses. Thus the overall efficiency of the solar system is increased.

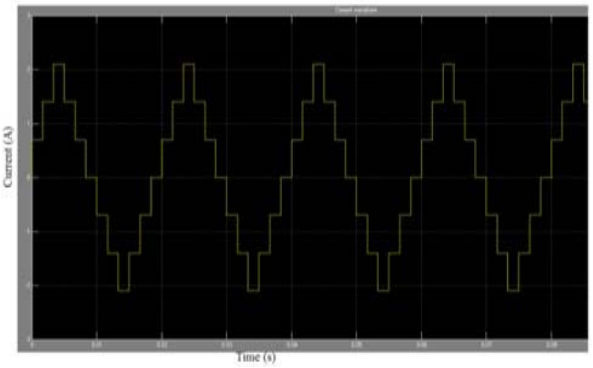

Figure-19. Current waveform of 7-level inverter.

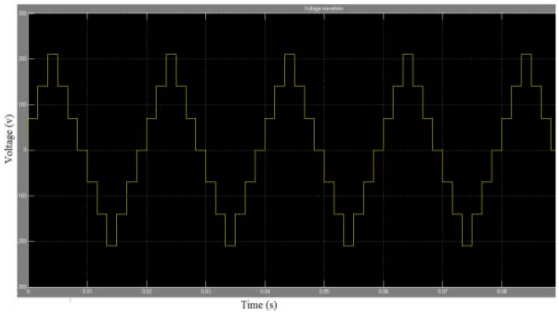

Figure-20. Voltage waveform of 7-level inverter.

CONCLUSIONS

This paper presents a control strategy of MPPT for the PV system, a modified SEPIC converter and a modified H-bridge inverter. The proposed algorithm for the solar panel to utilize maximum power irrespective of radiation level. The proposed algorithm effectively tracks the global optima of power value. Efficiency of the system is further increased by seven level inverter configurations with novel PWM switching scheme. So the control algorithm can be used in grid connected system used for grid connected system using other multilevel inverter topologies. This topology proves to be more efficient in both cost and gain. Losses are highly reduced with proposed inverter model. The method can very well be extended to several PV systems connected in series or parallel.

REFERENCES

[1] Roger Gules, Member, IEEE, Walter Meneghette dos Santos, Flavio Aparecido dos Reis, "A Modified SEPIC Converter With High Static Gain for Renewable Applications" IEEE transactions on power electronics, vol. 29, no. 11, Nov 2014.

[2] C. W. Li and X. He, "Review of non-isolated high step-up DC/DC converters in photovoltaic grid-connected applications," IEEE Trans. Ind.Electron., vol. 58, no. 4, pp. 1239–1250, Apr. 2011.

[3] S. B. Kjaer, J. K. Pedersen, and F.Blaabjerg, "A review of single-phase grid connected inverters for photovoltaic modules," IEEE Trans. Ind. Appl., vol. 41, no. 5, pp. 1292– 1306, Sep./Oct. 2005.

[4] P. K. Hinga, T. Ohnishi, and T. Suzuki, "A new PWM inverter for photovoltaic power generation system," in Conf. Rec. IEEE Power Electron. Spec. Conf., 1994, pp. 391–395.

[5] Y. Cheng, C. Qian, M. L. Crow, S. Pekarek, and S. Atcitty, "A comparison of diode-clamped and cascaded multilevel converters for a STATCOM with energy storage," IEEE Trans. Ind. Electron., vol. 53, no. 5, pp. 1512–1521, Oct. 2006.

[6] S. Alepuz, S. Busquets-Monge, J. Bordonau, J. A. M. Velasco, C. A. Silva, J. Pontt and J. Rodríguez, "Control strategies based on sym- metrical components f o r grid-connected c o n v e r t e r s u n d e r voltage dips," IEEE Trans. Ind. Electron. vol. 56, no. 6, pp. , Jun. 2009.

[7] J. Rodríguez, J. S. Lai, and F. Z. Peng, "Multilevel inverters: A survey of topologies, controls, and applications," IEEE Trans. Ind. Electron., vol. 49, no. 4, pp. 724–738, Aug. 2002.

[8] R. Stala, S. Pirog, M. Baszynski, A. Mondzik, A. Penczek, J. Czekonski, and S. Gasiorek, "Results of investigation of multicell converters with balancing circuit" IEEE Trans.
Ind. Electron, vol. 56, no. 7, pp. 2610–2619, Jul2009.

[9] J. Huang and K. A. Corzine, "Extended operation of flying capacitor multilevel inverter," IEEE Trans. Power Electron., vol. 21, no. 1, pp. 140–
147, Jan. 2006.

[10] G. Ceglia, V. Guzman, C. Sanchez, F. Ibanez, J. Walter, and M. I. Gimanez, "A new simplified multilevel inverter topology for DC–AC conversion," IEEE Trans. Power Electron., vol. 21, no. 5, pp. 1311–1319, Sep. 2006.

[11] Q. Zhao and F. C. Lee, "High-efficiency, high step-up DC– DC converters," IEEE Trans. Power Electron., vol. 18, no. 1, pp. 65–73, Jan. 2003
.

[12] M. F. Escalante, J.-C. Vannier, and A. Arzandé, "Flying capacitor multilevel inverters and DTC motor drive applications," IEEE Trans. Ind. Electron., vol. 49, no. 4, pp. 809–815, Aug. 2002.

[13] D. Zhou, A. Pietkiewicz, and S. Cuk, "A Three-Switch high- voltage converter,"IEEE Trans. Power Electron., vol. 14, no. 1, pp. 177–183, Jan.1999.

[14] M. Prudente, L. L. Pfitscher, G. Emmendoerfer, E. F. Romaneli, andR. Gules, "Voltage multiplier cells applied to non-isolated DC–DC converters,"IEEE Trans. Power Electron., vol. 23, no. 2, pp. 871–887, Mar.2008.

[15] V. G. Agelidis, D. M. Baker, W. B. Lawrance, and C. V. Nayar, "A multilevel PWM inverter topology for photovoltaic applications," in Proc. IEEE ISIE, Guimäes, Portugal, 1997, pp. 589–594.